Regulatory roles of ACSL5 in the anti-tumor function of palmitic acid (C16:0) *via* the ERK signaling pathway

Jiapei Lv,[1] Yanting Wang,[2] Shan Wei[1]

[1]The Affiliated People's Hospital of Ningbo University, Ningbo, Zhejiang
[2]Ningbo Zhenhai People's Hospital, Ningbo, Zhejiang, China

ABSTRACT

Previous studies have highlighted the susceptibility of cancer to perturbations in lipid metabolism. In particular, C16:0 has emerged as a promising novel treatment for hepatocellular carcinoma. In our study, we investigated the levels of C16:0 in the serum of non-small lung cancer patients were significant downregulation compared to healthy individuals (n=10; $p<0.05$). Moreover, our *in vitro* experiments using A549 cells demonstrated that C16:0 effectively inhibited proliferation, apoptosis, migration, and invasion. Despite these promising results, its pathogenesis remains poorly understood. CCK-8 assay, annexin V-FITC/PI double staining assay, wound healing assay and transwell assay were performed to evaluate the effects of C16:0, on proliferation, apoptosis, migration and invasion of A549 cells. RNA sequencing was used to identify essential factors involved in C16:0-growth inhibition in lung cancer. Further, the expression levels of related gene and proteins were detected by quantitative RT-PCR and Western blotting. Mouse NSCLC subcutaneous xenograft tumor model was established, and gastric lavage was given with C16:0. Tumor volume assay and hematoxylin-eosin staining were used to detect tumor growth *in vivo*. Our analysis revealed a significant upregulation of ACSL5 and its associated proteins in C16:0-treated A549 cells compared to the control group both *in vivo* and *in vitro*. Moreover, the knockdown of ACSL5 reversed the anti-tumor effect, resulting in an increased rate of the malignant phenotype mentioned above. Additionally, the expression of phosphorylated ERK protein was significantly inhibited with increasing concentrations of C16:0 in A549 cells. These results reveal for the first time that C16:0, as a novel target, regulates ACLS5 through the ERK signaling pathway, to inhibit the proliferation and apoptosis and inhibits cell migration and invasion of NSCLC. These findings may lead to the development of a novel therapeutic approach for non-small lung cancer.

Key words: non-small lung cancer; palmitic acid (C16:0); Acyl-CoA synthase long chain family member 5; ERK signal pathway.

Correspondence: Jiapei Lv, MD, The Affiliated People's Hospital of Ningbo University, No. 251, Baizhang Road, Ningbo, Zhejiang 315200, China. E-mail: lvjiapei_123@163.com

Contributions: all the authors made a substantive intellectual contribution, read and approved the final version of the manuscript and agreed to be accountable for all aspects of the work.

Conflict of interest: the authors declare that they have no competing interests, and all authors confirm accuracy.

Ethics Approval: this study was approved by the Animal Ethics Committee of Ningbo University (No. 2019-107).

Funding: this work was supported by the Natural Science Foundation of Zhejiang Province (LQ20H160010), the Medical and Health Research Project of Zhejiang Province (2023RC270), the Ningbo Key Discipline Construction Project (2022-B19), and the Ningbo Natural Science Foundation (2023J387).

Introduction

Lipids are critical components in cells, tissues, organs, and the body, playing a significant role in metabolism, structure, and energy supply. The development of mass spectrometry technology has led to the emergence of lipidomics as an emerging field in metabolomics.[1] Recent studies have shown that lipids contribute to tumor proliferation and metastasis, with dysregulated lipid metabolism considered a hallmark of malignant tumors.[2] Disorders in lipid metabolism have been observed in various types of cancers, including breast,[3] liver,[4] colorectal,[5] and lung cancer.[6] Consequently, lipids hold promise as potential biological markers for tumor diagnosis and treatment.

Lung cancer is a highly lethal malignancy worldwide, characterized by increasing incidence and poor prognosis.[7] To gain a better understanding of the regulatory mechanisms of the lipidomic spectrum in different lung cancer subtypes, the serum lipids of healthy individuals and lung cancer patients with adenocarcinoma (ADC), squamous cell carcinoma (SCC), and small cell lung cancer (SCLC) have been investigated. The results revealed significant differences in circulating levels of phosphatidylserine (PS) and lysoPS, which were considerably increased in lung cancer patients, while phosphatidylethanolamine (PE) and lysoPE levels were reduced. Moreover, specific lipids associated with different lung cancer subtypes were identified, exhibiting up- or down-regulation in SCC, ADC, or SCLC. These findings underscore the distinct lipid profiles of lung cancer patients compared to healthy individuals, as well as the subtype-specific differences in lipid composition.[8] To further explore the genomic landscape of lipid-related enzymes and proteins, our previous study integrated data from large-scale genomic screens and global mutation databases. It revealed significant differences in lipid-protein-related genes across various cancer subtypes, including the ACOT, ACSL, and PDK gene families, which are associated with alterations in lipid metabolite species and spatial structure.[8] Additionally, although the levels of palmitic acid (C16:0) were significantly reduced in non-small cell lung cancer (NSCLC) samples, several long-chain fatty acids (carbon atoms >40) were upregulated in lung cancer.[8] Notably, when C16:0 was added to the culture medium of lung cancer cells, the growth of these cells was significantly inhibited, indicating C16:0 as a potential targeted lipid in NSCLC. Subsequent RNA sequencing identified Acyl-CoA Synthetase Long-Chain Family Member 5 (ACSL5) as a molecular marker whose expression was dramatically increased in lung cancer cells stimulated by C16:0, up to 20 times higher than the control group.[9] Based on these findings, we hypothesized that ACSL5 is strongly associated with the incidence and progression of NSCLC.

Free fatty acids can be directed towards anabolic or catalytic pathways through ATP-dependent reactions catalyzed by ACSLs.[10] Among the ACSL gene family, ACSL5 plays a significant role in transforming free long-chain fatty acids with 12-22 carbons into acyl-CoA esters.[10] Dysregulation of ACSL genes, including ACSL5, has been observed in various human cancers and contributes to their transformation. Abnormal expression of ACSL5 has been implicated in the occurrence and progression of several cancer types.[11] Moreover, the expression of ACSL5, acting as either a carcinogenic or tumor suppressor factor, is influenced by a variety of factors depending on the specific cancer type or subtype.[12] We aimed to investigate the inhibitory effect of C16:0 on NSCLC through *in vivo* and *in vitro* experiments and the relationship between C16:0 and ACSL5.

Materials and Methods

Cell culture

The A549 line was obtained from the cell bank of the Chinese Academy of Sciences (Shanghai, China). Heat-inactivated fetal bovine serum (10%, Corning Cellgro, Mulgrave, Australia), 100 mg/mL streptomycin, and 100 U/ml penicillin were added to the cell culture medium DMEM (KeyGEN, Nanjing, China). Cells were incubated at 37°C in a humidified environment containing 5% CO_2, and passed down every 3 days.

Reagents and materials

C16:0 was purchased from Sigma-Aldrich (St. Louis, MO, USA) and dissolved in 1 mM NaOH and PBS containing BSA (10 mM). PrimeScript RT reagents and SYBR Premix Ex Taq (TaKaRa, Shiga, Japan) were used for RNA analysis. The anti-ACSL5 antibody was purchased from Santa Cruz Biotechnology, Inc. (Santa Cruz, CA, USA).

Cell proliferation and apoptosis measurement

To assess the sensitivity and response of A549 cells to C16:0 and selected targets, cell proliferation, apoptosis, migration, and invasion were measured. A total of 2×10^3 were seeded in each well of a 96-well plate and treated with C16:0 at concentrations of 50 μM, 100 μM, 200 μM, and 400 μM for 48 h, respectively. After treatment, 10% CCK-8 solution (Dojindo, Japan) was added to the cells in 90 μL DMEM, followed by an additional incubation of 1 or 2 h. The optical density (OD) value was measured at 450 nm using a Spectra Max®Absorbance Reader (CMax Plus; Molecular Devices, San José, CA, USA). Each experiment was repeated at least six times. Apoptotic cells were detected using an annexin V-FITC/PI double staining assay according to the manufacturer's instructions. Cells were plated at a density of 10^5 per well in a six-well plate and incubated with different concentrations of C16:0. After 48 h, cells were collected in binding buffer, stained with annexin-V-FITC (Miltenyi Biotec Inc, Bergisch Gladbach, Germany) for 15 min at room temperature, followed by PI for 5 min. The stained cells were immediately analyzed using a BD FACSCanto™ II flow cytometer (BD Bioscience, Franklin Lakes, NJ, USA). Each experiment was repeated at least six times.

Cell migration and invasion

Wound healing and transwell assays were employed to examine cell migration and invasion. Cells were seeded in 6-well culture plates, and after 48 h the cells are filled with plates, wounds are created on the cell monolayer using a 10 μL pipette, serum is removed to minimize the effects of cell proliferation. At this time, cells are treated with different concentrations of C16:0 (50 μM, 100 μM, 200 μM, 400 μM), measuring the movement of cells into the scratched area under a 10× objectives lens at 0, 24 and 48 h and determining the migration state. The healing rate was calculated by randomly selecting 6 sites per well for at least 3 repetitions. For cell invasion assessment, Matrigel (Corning Cellgro) was pre-coated on the chambers and allowed to solidify at 37°C for 2 h. Cells were digested, washed 1-2 times with PBS, and re-suspended in serum-free media with BSA. The cell density was adjusted to 5×10^5/mL, and 1×10^5 cells were seeded in the upper layer of the chamber, while DMED with 20% serum was added to the lower layer of the chamber. After 48 h, the cells were fixed with ethanol, the cells outside the chamber were wiped off, and the remaining cells were stained with 0.1% crystal violet for 30 min at room temperature. Each experiment was repeated at least three times. Cell counting was performed using ImageJ software.

Real-time PCR

Before RNA extraction, cells were rinsed with phosphate buffer. TRIzol reagent (500 µL) (Invitrogen, Carlsbad, CA, USA) was added to each well, followed by 200 µL of chloroform, and 200 µL of promethazine. After reverse transcription using PrimeScript RT Master Mix (TaKaRa), the mRNA of target genes was amplified using SYBR green fluorescence (TaKaRa). Quantitative RT-PCR was performed using an ABI 7500 Fast Real-Time PCR system (Applied Biosystems, ABI Life Technologies, Foster City, CA, USA), with the following program parameters: 2-min incubation at 95°C, followed by 40 cycles of 3 s at 95°C and 30 s at 60°C. The primer sequences used were as follows: Human β-actin: (forward) 5′-AGCGAGCATCCCCCAAAGTT-3′ and (reverse) 5′-GGGCACGAAGGCTCATCATT-3′; and human ACSL5, (reverse) 5′-CGTC AGCCAGCAACCGAATATCC-3′ and (forward) 5′-GTCATCTGCTTCACCAGTGG-3′. The $2^{-\Delta\Delta CT}$ method was used based on the threshold cycle (Ct) to calculate relative mRNA expression levels after normalization to the internal control (each measurement was repeated at least six times per group).

RNA interference

Three distinct ACSL5 siRNA sequences were created by GenePharma: ACSL5-Homo-1604: GCUUAUGGUCAAACAGAAUTT, AUUCUGUUUGACCAUAAGCTT; ACSL5-Homo-1509: GCGGAAGGGUUCGUGUAAUTT, AUUACACGAACCCUUCCGCTT; ACSL5-Homo-731: GCUUGUUACACGUACUCUATT, UAGAGUACGUGUAACAAGCTT. For each well, NC or siRNA at a concentration of 20 pmol per microliter was added to lipofectamine 2000 (Invitrogen) at room temperature for 20 min. Realtime PCR was used to detect mRNA expression after 24 h of interference at 37°C, allowing assessment of interference effectiveness. The ACSL5-Homo-731 sequence was selected as an efficient siRNA for stable transfection of ACSL5, and additional experiments were performed.

Western blot

A549 cell pellets were lysed on ice for 30 min using RIPA lysis buffer (strong, without inhibitors; Beyotime, Shanghai, China) supplemented with protease inhibitors (Beyotime). The total protein concentration was determined by measuring absorbance at 260 nm using a NanoDrop instrument (Thermo Fischer Scientific, Waltham, MA, USA). SDS-PAGE gel (EpiZyme, Shanghai, China) was used to separate 20 µg of protein, which was then transferred to a polyvinylidene difluoride (PVDF) membrane. The membrane was blocked with a blocking solution (Beyotime) for 15 min at room temperature on a shaker. Subsequently, the membrane was incubated overnight at 4°C with antibodies (anti-ACSL5, #sc-365478; Santa Cruz), (anti-Ki-67, #ab16667; Abcam, Cambridge, UK), (anti-p53, #ab131442; Abcam), all the three antibodies were diluted 1:1000. Following this, the membrane was incubated with a secondary antibody, IPKine HPR Mouse Anti-Rabbit IgG LCS (A25022), diluted 1:2000, for 1 h at room temperature. The membrane was washed three thrice times for a total of ten min each with PBS containing 0.1% Tween 20. Protein bands were visualized using Clarity™ Western ECL Substrate Transition Guide (Bio-Rad, Hercules, CA, USA) on a PVDF 0.45 µM Transfer Membrane (Immobilon®-p). Actin antibody (Abcam, Cambridge, MA, USA) was used as a protein loading control. Measurement was repeated at least six times per group.

In vivo assays for tumor growth

All experiments were approved by the Ningbo University Animal Care and Use Committee. Eight-week-old male BALB/C nude mice used in this study were purchased from the Experimental Animal Center of Southern Medical University (Guangzhou, China). The mice were housed in individually ventilated cages with a 12-h light-dark cycle and maintained at a temperature range of 19° to 23°C, with a standard meal provided. To investigate the potential of C16:0 in suppressing carcinogenesis *in vivo*, 1×107 A549 cells per 100 µL PBS were injected subcutaneously on the back of nude mice. When the tumor reached 30 mm^3, they are randomly divided into two groups (n=6): a control group and a C16:0-treated group. The treatment group used C16:0 10.26 mg/kg intraperitoneal injection per day, the control group was given the same amount of normal saline solution intraperitoneal injection. Tumor volumes were measured every three days using the formula $V=(length\times width^2)/2$ in mm^3. Animals were euthanized before tumor volumes reached 2000 mm^3. The experiment was terminated on day 28 after drug treatment, and tumor volume and weight were measured for subsequent histological examination.

Immunohistochemistry

Subcutaneous tumors were excised, fixed in 10% formalin for 24 h at room temperature, and embedded in paraffin. Serial sections are obtained from each tumor block to dewax and rehydrate all tissue slides. The slides are then incubated in 0.3% H_2O_2 methanol for 10 min to block endogenous peroxidase activity. Perform antigen retrieval with sodium citrate (pH=6) in an autoclave for 5 min. The slides are then dropwise supplemented with antibodies (anti-ACSL5, #ab272556, Abcam, host species: Rabbit, diluted at a ratio of 1:100; anti-Ki-67, #ab16667, Abcam, host species: Rabbit, dilution ratio is 1: 200; Anti-P53, #ab131442, Abcam, host species: Rabbit, dilution ratio 1:100) incubate overnight at 4°C. Slides not treated with primary antibodies serve as negative controls. The second day, incubate the secondary antibody (VectorLabs, Newark, CA, USA; #BA1000, dilution ratio 1:200) at room temperature for 45 min and observe with DBA solution for color development, followed by counterstaining with hematoxylin for 1 min. Take pictures of the cover after cleaning. Quantitative measurement of the immunopositivity used ImageJ software.

Results

Effect of C16:0 on cells and biological behaviors

The effect of different concentrations of C16:0 on A549 cells was investigated, revealing a significant dose-dependent inhibition of cell proliferation (Figure 1A) ($p<0.05$ or less, respectively). After 48 h of C16:0 treatment, the migration of A549 cells was assessed, demonstrating that C16:0 effectively suppressed cell migration (Figure 1B). Additionally, the apoptotic rate of A549 cells significantly increased following treatment with C16:0 for 48 h, with the highest dose resulting in a threefold increase compared to the control group. Moreover, treatment of A549 cells with 200 µM C16:0 for 48 h led to approximately 50% inhibition of invasive capacity (Figure 1 D,E).

Verification of ACSL family expression

The gene expression of ACSL1, ACSL3, ACSL4, ACSL5, ACSL6 in A549 cells treated with different concentrations (50 µM, 100 µM, 200 µM) of C16:0 at 24 h and 48 h is presented in Figure 2 A,B ($p<0.05$ or less). Specifically, the expression of the ACSL5 gene in A549 cells significantly increased after treatment with C16:0 at concentrations ranging from 50 µM to 200 µM for 48 h. The ACSL5 expression levels were more than 20-fold higher than the control group when the concentration of C16:0 reached 200

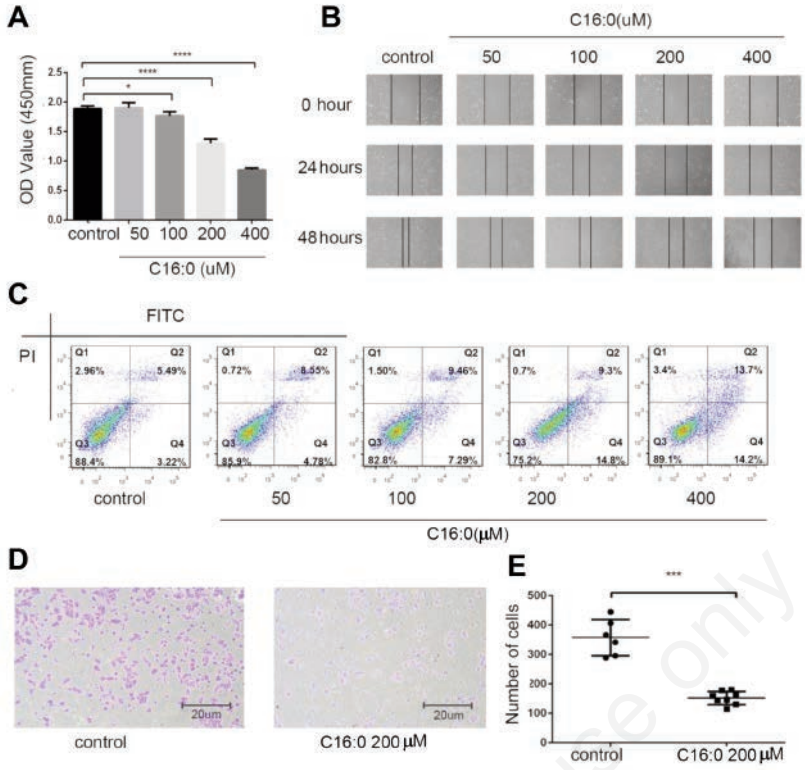

Figure 1. Functional effects of c16:0 on non-small cell lung cancer. A-C) Impact of C16:0 on A549 cells at four different doses (50 μM, 100 μM, 200 μM, 400 μM) after 48 h of treatment; cell proliferation (**A**), cell migration (**B**), and apoptosis (**C**) were assessed. **D**) Invasion of A549 cells stimulated with 200 μM C16:0 for 48 h compared to the control group. **E**) Quantification of invasive cells in each microscope field. *p<0.05, ***p<0.001, ****p<0.001, compared to controls.

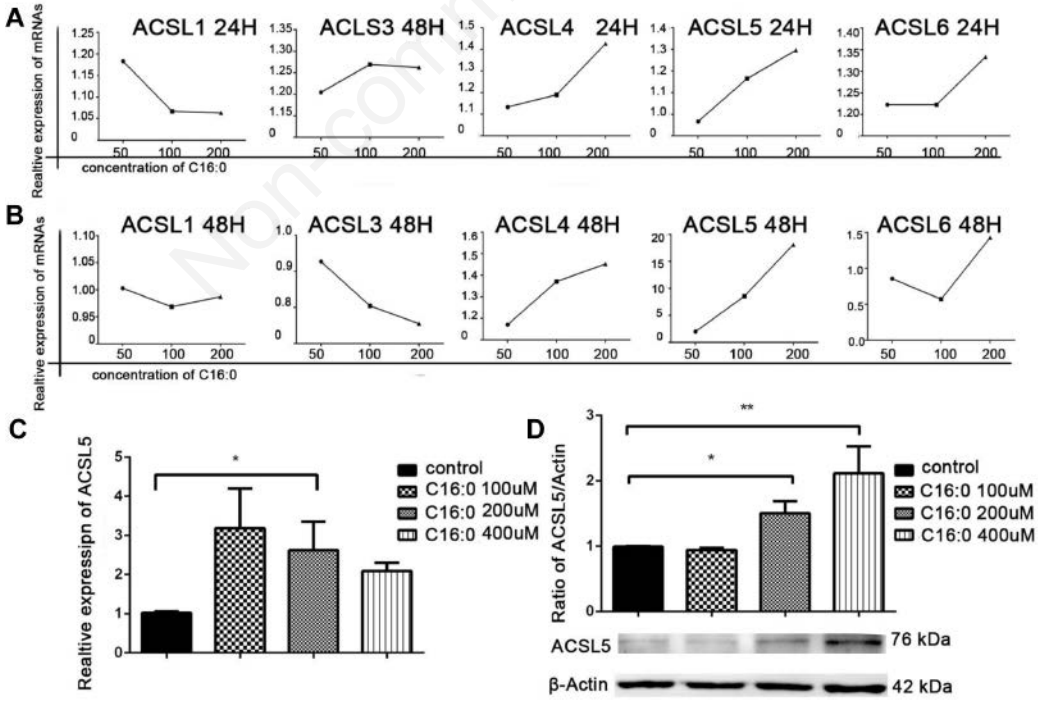

Figure 2. C16:0-induced ACSL5 mRNA and protein expression. **A,B**) Expression of ACSL family genes after treatment with different concentrations (50 μM, 100 μM, 200 μM) of C16:0 at 24 h (**A**) and 48 h (**B**). **C,D**) Assessment of ACSL5 RNA expression (**C**) and protein expression (**D**) in A549 cells stimulated with C16:0 for 48 h. *p<0.05, **p<0.01, compared to controls.

μM. However, there was little difference in the expression of other ACSL family members after treatment with C16:0. Furthermore, we assessed the expression levels of ACSL5 mRNA in A549 treated with C16:0 concentrations ranging from 100 μM to 400 μM using qRT-PCR. The data indicated a significant increase in expression only when the C16:0 concentration reached 200 μM (Figure 2C). Additionally, we examined the protein levels of ACSL5 after treatment with C16:0 concentrations ranging from 50 to 200 μM. As shown in Figure 2D, the protein expression levels increased with the concentration of C16:0.

C16:0 inhibits xenograft growth *in vivo* and reduces malignancy

To further investigate the effect of C16:0 on tumor development *in vivo*, we established a xenograft tumor model by subcutaneously injecting A549 cells into nude mice. Consistent with the results of our previous cell experiments, C16:0 exhibited a significant inhibitory effect on tumor growth (Figure 3 A,B). Immunohistochemistry was performed to measure the expression levels of ACSL5, Ki67, and P53 in the mice tumor tissues. As expected, the results showed an upregulation of ACSL5 and P53 expression in the C16:0 treated group (Figure 3 D,E), while the levels of Ki67 were reduced compared to the control group (Figure 3C). Additionally, Western blot analysis was performed to evaluate the change in ACSL5 expression, and the data were consistent with our *in vitro* results, demonstrating a higher protein level of ACSL5 in the treatment group (Figure 3F). These findings reaffirm the effect of C16:0 on NSCLC and suggest that ACSL5 may play a crucial role in this process.

ACSL5 is identified as a master regulator in the molecular network of C16:0-treated non-small lung cancer cells

Given the elevated expression of ACSL5 in NSCLC and its close correlation with disease development, we investigated whether ACSL5 might be involved in NSCLC pathogenesis and serve as a novel therapeutic target. To this end, we used siRNA transfection to knockdown ACSL5. Three siRNAs were used to interfere with A549 cells and verify ACSL5 expression by PCR. Among them, the inhibitory efficiency of ACSL5-homo-731 was close to 90%, the inhibitory efficiency of ACSL5-homo-1509 was 56%, and ACSL5-homo-1840 had no obvious effect (Figure 4A). Therefore, ACSL5-homo-731 was screened as a valid ACSL5 siRNA sequence and stable ACSL5 knockdown cells were established (Figure 4A). Firstly, we confirmed the reduced RNA and protein expression levels of ACSL5 in the knockdown group compared to the control group using RT-PCR and Western blotting, respectively (Figure 4 B,C). Additionally, we observed that C16:0

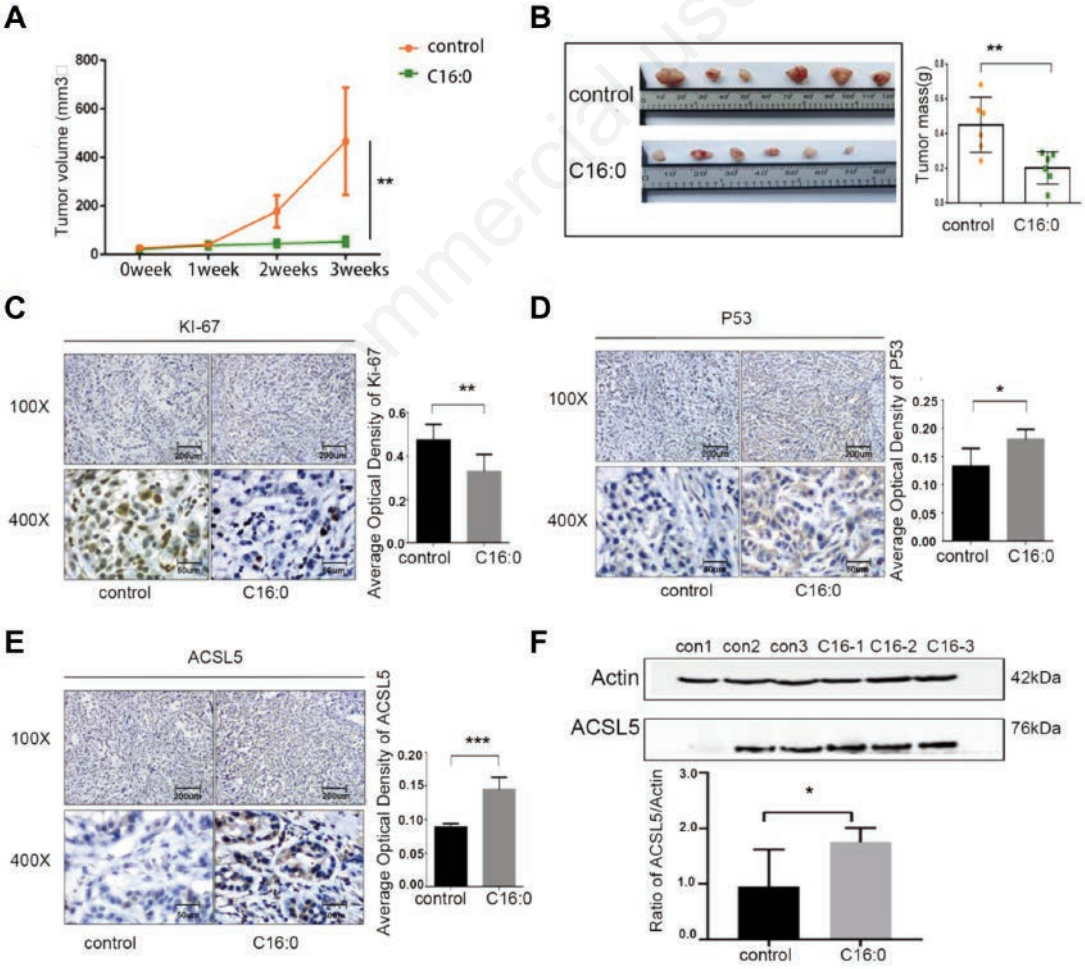

Figure 3. Biological implications of C16:0 in tumorigenesis *in vivo*. **A**) Comparison of cell proliferation rates in A549 xenografts following subcutaneous injection of C16:0 compared to controls. **B**) Comparison of the growth of A549 xenografts following subcutaneous injection of C16:0 compared to controls. **C-E**) Expression of ki-67 (**C**), P53 (**D**), and ACSL5 (E) in C16:0-treated xenografts compared to controls. **F**) Western blot analysis of ACSL5 expression in A549 xenografts. *p<0.05, **p<0.01, ***p<0.001, compared to controls.

increased the expression of ACSL5, while no similar result was observed in the siRNA-731+C16:0 group. Next, to evaluate the effect of ACSL5 knockdown on cell growth, we performed CCK8 analyses. We found that C16:0 lost its ability to inhibit A549 cell proliferation when cells were transfected with siRNA (Figure 4D). Furthermore, to investigate whether ACSL5 knockdown could inhibit A549 migration, we conducted a wound healing assay. The dosing group exhibited a significant decrease in migration rate compared to the control cells. However, the migratory capacity of A549 cells in the transfection group was similar to that of the control group (Figure 4E). Overall, these results demonstrate that C16:0 inhibits proliferation and migration in NSCLC cells through its regulation of ACSL5 expression.

ACSL5 involvement in the specific regulation of the ERK signaling pathway

To investigate the mechanism by which C16:0 inhibits lung cancer development, we stimulated A549 cells with different concentrations of C16:0 for 2 h and examined the tumor proliferation-related pathways, ERK, and AKT signaling pathways. We observed that as the concentration of C16:0 increased, the phosphorylation of ERK, a protein associated with tumor growth, was inhibited, while the phosphorylation of AKT did not show significant changes. These findings indicate that C16:0 may inhibit NSCLC through the ERK pathway (Figure 5A). However, further exploration is needed to understand how C16:0 regulates the phosphorylation of downstream pathways. We then performed Western blot analysis to assess the expression changes of p-ERK and p-AKT. We observed that the phosphorylation of ERK was markedly enhanced in ACSL5 knock-down cells, and C16:0 no longer inhibited p-ERK expression in these cells as shown in Figure 5B. On the other hand, the protein level of p-AKT was not statistically affected by ACSL5 knockdown or C16:0 addition. These results provide further confirmation that C16:0 inhibits NSCLC progression by activating the ERK pathway, and this process may be mediated by the upregulation of ACSL5 (Figure 6).

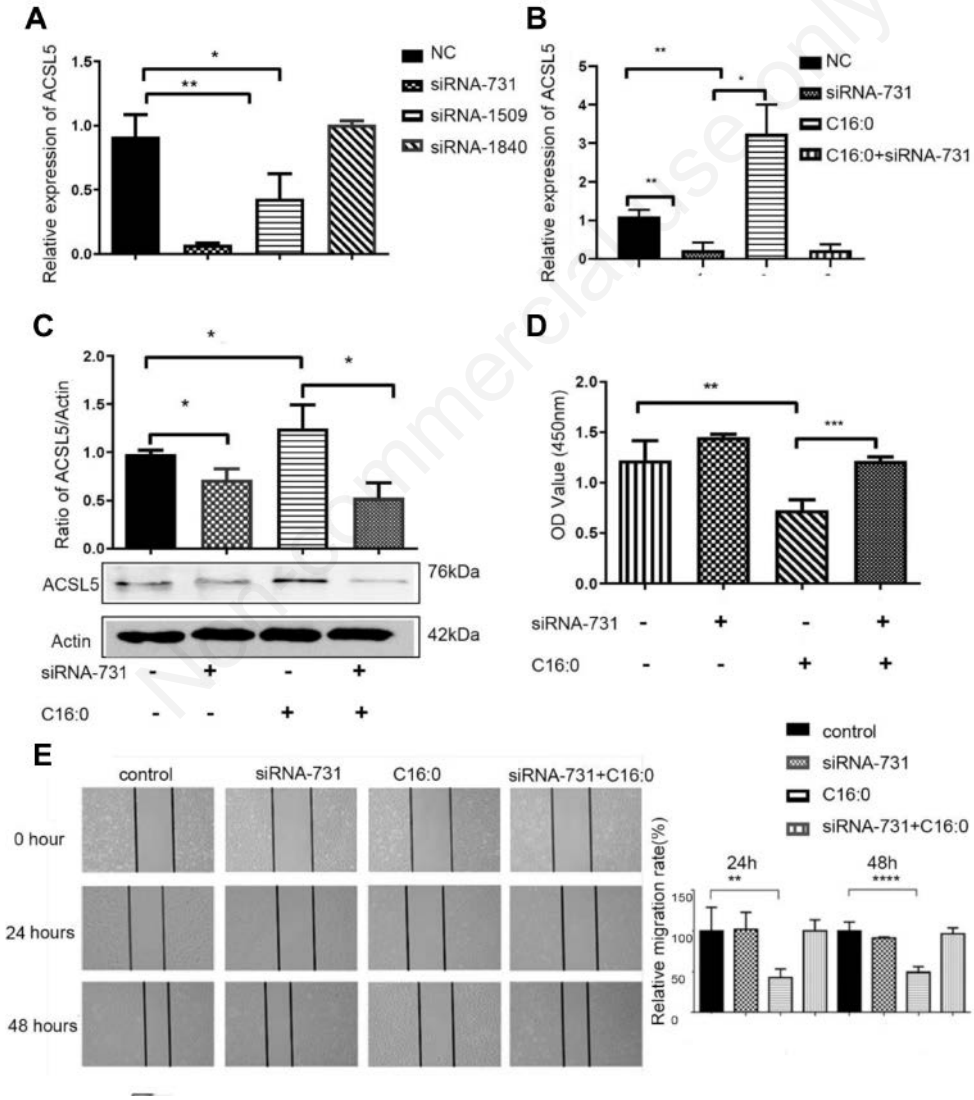

Figure 4. Effect of C16:0 on ACSL5-negative lung cancer cell function and key pathway. **A**) Changes in ACSL5 mRNA were observed with siRNA-731 and siRNA1509 treatment in A549 cells for 24 h. **B,C**) ACSL5 siRNA-731 decreased the expression of the ACSL5 gene and inhibited the upregulation of ACSL5 mRNA (**B**) and protein (**C**) levels after treatment with 200 μM C16:0 for 48 h, $p<0.01$ or less, respectively. **D,E**) Evaluation of ACSL5-negative A549 cell responses to 200 μM C16:0 compared to controls; cell proliferation (**D**), and migration (**E**) were assessed. *$p<0.05$ or less compared to controls.

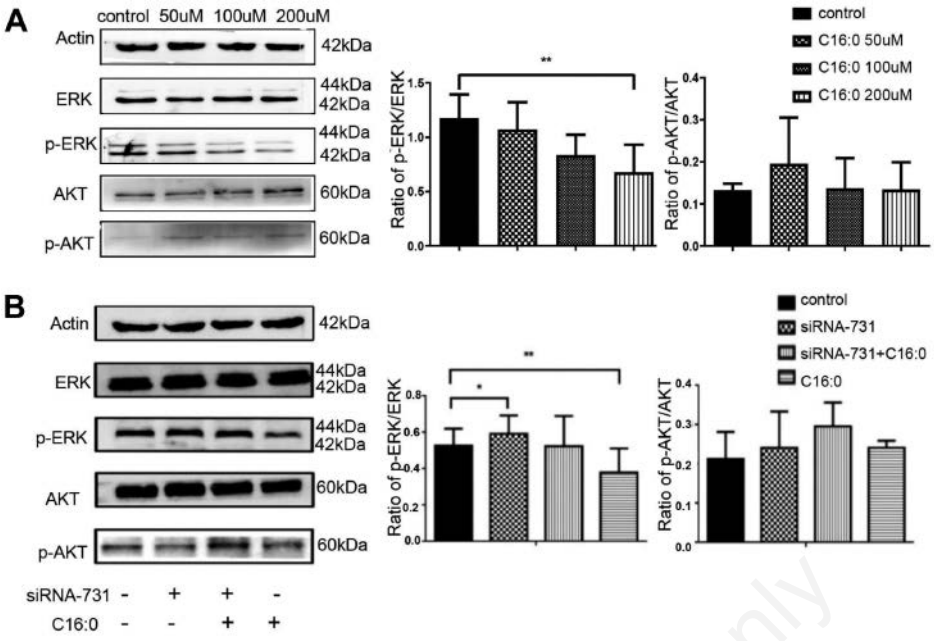

Figure 5. Identification of ACSL5-mediated downstream pathways. **A**) Western blot analysis of ERK and AKT phosphorylation in A549 cells treated with different doses of C16:0 for 2 h. **B**) The phosphorylation status of AKT and ERK pathways in A549 cells after ACSL5 knockdown. *p<0.05, **p<0.01, ***p<0.001, compared to controls.

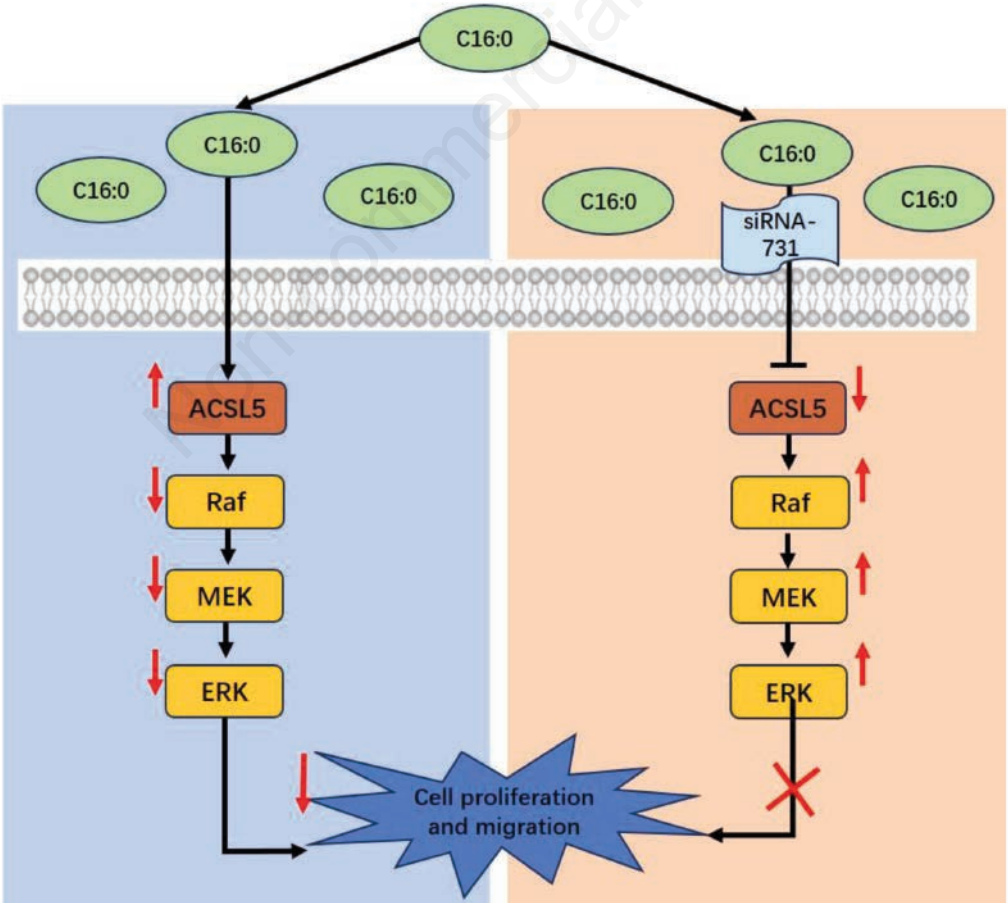

Figure 6. Exogenous C16:0 inhibited lung cancer cell proliferation and migration by ACSL5/ERK pathway. When ACSL5 was inhibited, lung cancer cells were insensitive to C16:0.

Discussion

Lipids, as crucial components of cellular membranes, play important roles in numerous cellular processes, including cell growth, proliferation, differentiation, and signaling.[13] Disturbances in lipid metabolism can occur in both non-carcinogenic and oncogenic states, affecting cellular function. The emergence of liquid mass spectrometry has facilitated the study of tumors through lipidomics.[14] Studies have demonstrated significant differences in certain PC and PE levels in the plasma of early-stage NSCLC patients compared to healthy individuals. For instance, PE (18:0/18:1), PE (20:5/18:1), PE (18:1/20:4), PC (15:0/18:1), PC (16:1/20:5), and PC (18:0/20:1) were found to be elevated in the plasma of NSCLC patients.[15] Conversely, a small proportion of hemolytic PC species containing fatty acids18:2, 18:1, and 18:0 were significantly downregulated in the plasma of NSCLC patients.[16] Our findings revealed that plasma lipids in NSCLC patients exhibited heterogeneity compared to those in healthy individuals, specifically showing significantly lower levels of palmitic acid (C16:0) content.[8] Aberrant C16:0 metabolism has also been observed in other cancers, such as melanoma,[17] and hepatocellular carcinoma.[18] Further investigation revealed that C16:0 inhibited the proliferation of multiple non-small lung cancer cell lines.[9] Therefore, we speculate that C16:0 metabolism may play an important role in tumorigenesis, although research on the specific molecular processes through which C16:0 contributes to the development of those diseases, particularly cancer, remains limited.

ACSL5 is a member of the long-chain Acyl-CoA synthase (ACSLs) family and is known to participate in intestinal cell differentiation and maturation by regulating the proliferation and apoptosis of intestinal cells.[19] Abnormal expression of ACSL5 has been strongly associated with colorectal cancer, glioma, and other cancers.[20] ACSL5 also holds potential prognostic value in various tumors. For example, it has been identified as an independent prognostic marker for early recurrence in sporadic colorectal adenocarcinoma.[21] High expression of ACSL5 is associated with better prognosis in both ER-positive and ER-negative breast cancer patients.[22] Additionally, downregulation of ACSL5 expression has been observed in pancreatic cancer patients with good prognoses.[23] In normal cells, fatty acids can regulate the expression of ACSL, and it is hypothesized that a similar mechanism may be involved in the dysregulation of ACSL in tumor cells. Abnormal control of lipid metabolism is also associated with poor survival in cancer patients.[24] In our study, we found low expression of ACSL5 in A549 cells, but after treatment with different concentrations of C16:0, the expression level of ACSL5 increased, suggesting that C16:0 can regulate the growth, migration, and apoptosis of A459 cells through ACSL5.

The abnormal expression of signal transduction pathways in lung cancer forms the basis for the development of small-molecule targeted drugs for lung cancer therapy. Among these pathways, the ERK pathway plays an important role in endothelium signaling. Activation of the substrate ERK is a critical step in transmitting cell surface receptor signals to the nucleus.[25] ERK is a serine/threonine protein kinase that, when phosphorylated ERK1/2, can activate nuclear transcription factors, cytosolic proteins, and kinases. This activation leads to increased secretion of VEGF secretion and enhanced tumor growth capacity.[26] In our study, we observed a significant decrease in p-ERK levels in A549 cells treated with palmitic acid ($p<0.05$), suggesting that PA may exert its effects by inhibiting the activation of the ERK pathway.

The limitation of this study is although we have previously identified the heterogeneity of C16:0 in the serum of human lung cancer patients, there was no carefully described prognosis, treatment effect, and whether C16:0 levels are associated with ACSL5 expression in tumor tissues. Further research needs to expand the sample size to explore the difference between C16:0 in lung cancer and healthy people or other chronic lung diseases. Determine the location of C16:0 in lung tissue, especially in malignant or paracancerous tissues.

In conclusion, this study provides compelling preclinical evidence that C16:0 can effectively inhibit the growth and metastasis of lung cancer through the ACSL5-ERK signal pathway. Through *in vivo* and *in vitro* experiments, we demonstrated that exposure to different concentrations of C16:0 leads to the inhibition of proliferation, migration, and invasion of NSCLC cells while promoting apoptosis. We identified and validated the critical role of the ACSL5 gene as the primary regulator in the molecular networks of C16:0-treated lung cancer cells. The involvement of the ERK signaling pathway was observed in mediating the sensitivity of lung cancer cells to C16:0, highlighting the significance of ACSL5 in this process. These findings suggest that ACSL5 may play a critical role in determining the susceptibility of lung cancer cells to C16:0 and could potentially contribute to the development of drug resistance. Our research supported the viewpoint that C16:0 composition is causally related to the regulation of NSCLC growth and metastasis, and provides opportunities for diagnosing and treating NSCLC by targeting the altered C16:0 metabolism in the near future.

References

1. Lv J, Zhang F, Wang X. Clinical lipidomics: a new way to diagnose human diseases. Clin Transl Med 2018; 7: 12.
2. Snaebjornsson MT, Janaki-Raman S, Schulze A. Greasing the wheels of the cancer machine: the role of lipid metabolism in cancer. Cell Metab 2020;31:62-76.
3. Doria ML, Cotrim Z, Macedo B, Simoes C, Domingues P, Helguero L, et al. Lipidomic approach to identify patterns in phospholipid profiles and define class differences in mammary epithelial and breast cancer cells. Breast Cancer Res Tr 2012;133:635-48.
4. Bu SY, Mashek DG. Hepatic long-chain acyl-CoA synthetase 5 mediates fatty acid channeling between anabolic and catabolic pathways. J Lipid Res 2010;51:3270-80.
5. Fhaner CJ, Liu S, Ji H, Simpson RJ, Reid GE. Comprehensive lipidome profiling of isogenic primary and metastatic colon adenocarcinoma cell lines. Anal Chem 2012;84:8917-26.
6. Ren J, Zhang D, Liu Y, Zhang R, Fang H, Guo S, et al. Simultaneous quantification of serum nonesterified and esterified fatty acids as potential biomarkers to differentiate benign lung diseases from lung cancer. Sci Rep 2016;6:34201.
7. Siegel RL, Miller KD, Fuchs HE, Jemal A. Cancer statistics, 2021. CA Cancer J Clin 2021;71:7-33. Erratum in: CA Cancer J Clin 2021;71:359.
8. Lv J, Gao D, Zhang Y, Wu D, Shen L, Wang X. Heterogeneity of lipidomic profiles among lung cancer subtypes of patients. J Cell Mol Med 2018;22:5155-9.
9. Zhang L, Lv J, Chen C, Wang X. Roles of acyl-CoA synthetase long-chain family member 5 and colony stimulating factor 2 in inhibition of palmitic or stearic acids in lung cancer cell proliferation and metabolism. Cell Biol Toxicol 2021;37:15-34.
10. Soupene E, Kuypers FA. Mammalian long-chain acyl-CoA synthetases. Exp Biol Med 2008;233:507-21.
11. Chen WC, Wang CY, Hung YH, Weng TY, Yen MC, Lai MD. Systematic Analysis of gene expression alterations and clinical outcomes for long-chain acyl-coenzyme A synthetase family in cancer. Plos One 2016;11:e155660.
12. Hartmann F, Sparla D, Tute E, Tamm M, Schneider U, Jeon

MK, et al. Low acyl-CoA synthetase 5 expression in colorectal carcinomas is prognostic for early tumour recurrence. Pathol Res Pract 2017;213:261-6.
13. Wit M, Trujillo-Viera J, Strohmeyer A, Klingenspor M, Hankir M, Sumara G. When fat meets the gut-focus on intestinal lipid handling in metabolic health and disease. Embo Mol Med 2022;14:e14742.
14. Hsu FF. Mass spectrometry-based shotgun lipidomics - a critical review from the technical point of view. Anal Bioanal Chem 2018;410:6387-409.
15. Chen Y, Ma Z, Shen X, Li L, Zhong J, Min LS, et al. Serum lipidomics profiling to identify biomarkers for non-small cell lung cancer. Biomed Res Int 2018;2018:5276240.
16. Ros-Mazurczyk M, Jelonek K, Marczyk M, Binczyk F, Pietrowska M, Polanska J, et al. Serum lipid profile discriminates patients with early lung cancer from healthy controls. Lung Cancer 2017;112:69-74.
17. Liu R, Cao K, Tang Y, Liu J, Li J, Chen J, et al. C16:0 ceramide effect on melanoma malignant behavior and glycolysis depends on its intracellular or exogenous location. Am J Transl Res 2020;12:1123-35.
18. Lin L, Ding Y, Wang Y, Wang Z, Yin X, Yan G, et al. Functional lipidomics: Palmitic acid impairs hepatocellular carcinoma development by modulating membrane fluidity and glucose metabolism. Hepatology 2017;66:432-48.
19. Diebels I, Van Schil P. Diagnosis and treatment of non-small cell lung cancer: current advances and challenges. J Thorac Dis 2022;14:1753-7.
20. Min L, Zhu T, Lv B, An T, Zhang Q, Shang Y, et al. Exosomal LncRNA RP5-977B1 as a novel minimally invasive biomarker for diagnosis and prognosis in non-small cell lung cancer. Int J Clin Oncol 2022;27:1013-24.
21. Guo L, Li L, Xu Z, Meng F, Guo H, Liu P, et al. Metabolic network-based identification of plasma markers for non-small cell lung cancer. Anal Bioanal Chem 2021;413:7421-30.
22. Wang J, Zhang L, Wang C, Chen Y, Sui X. LINC00313/miR-4429 axis provides novel biomarkers for the diagnosis and prognosis of non-small cell lung cancer. Acta Biochim Pol 2022;69:343-8.
23. Fatima S, Hu X, Gong RH, Huang C, Chen M, Wong H, et al. Palmitic acid is an intracellular signaling molecule involved in disease development. Cell Mol Life Sci 2019;76:2547-57.
24. Bai D, Wu Y, Deol P, Nobumori Y, Zhou Q, Sladek FM, et al. Palmitic acid negatively regulates tumor suppressor PTEN through T366 phosphorylation and protein degradation. Cancer Lett 2021;496:127-33.
25. Li J, Fan Y, Zhang Y, Liu Y, Yu Y, Ma M. Resveratrol induces autophagy and apoptosis in non-small-cell lung cancer cells by activating the NGFR-AMPK-mTOR pathway. Nutrients 2022;14:2413.
26. Tang G, Zeng Z, Sun W, Li S, You C, Tang F, et al. Small nucleolar RNA 71A promotes lung cancer cell proliferation, migration and invasion via MAPK/ERK pathway. J Cancer 2019;10:2261-75.

Received: 9 September 2023. Accepted: 24 October 2023.

European Journal of Histochemistry 2023; 67:3867
doi:10.4081/ejh.2023.3867